Voltage-Dependent Modulation of Single N-Type Ca^{2+} Channel Kinetics by Receptor Agonists in IMR32 Cells

V. Carabelli,* M. Lovallo,* V. Magnelli,* H. Zucker,‡ and E. Carbone*
*Dipartimento di Neuroscienze, Corso Raffaello 30, I-10125 Torino, Italy, and ‡Max-Planck-Institut für Psychiatrie, Am Klopferspitz 18A, D-8044 Planegg, Germany

ABSTRACT The voltage-dependent inhibition of single N-type Ca^{2+} channels by noradrenaline (NA) and the δ-opioid agonist D-Pen_2-D-Pen_5-enkephalin (DPDPE) was investigated in cell-attached patches of human neuroblastoma IMR32 cells with 100 mM Ba^{2+} and 5 μM nifedipine to block L-type channels. In 70% of patches, addition of 20 μM NA + 1 μM DPDPE delayed markedly the first channel openings, causing a four- to fivefold increase of the first latency at +20 mV. The two agonists or NA alone decreased also by 35% the open probability (p_o), prolonged partially the mean closed time, and increased the number of null sweeps. In contrast, NA + DPDPE had little action on the single-channel conductance (19 versus 19.2 pS) and minor effects on the mean open time. Similarly to macroscopic Ba^{2+} currents, the ensemble currents were fast activating at control but slowly activating and depressed with the two agonists. Inhibition of single N-type channels was effectively removed (facilitated) by short and large depolarizations. Facilitatory pre-pulses increased p_o significantly and decreased fourfold the first latency. Ensemble currents were small and slowly activating before pre-pulses and became threefold larger and fast decaying after facilitation. Our data suggest that slowdown of Ca^{2+} channel activation by transmitters is mostly due to delayed transitions from a modified to a normal (facilitated) gating mode. This single-channel gating modulation could be well simulated by a Monte Carlo method using previously proposed kinetic models predicting marked prolongation of first channel openings.

INTRODUCTION

Neuronal N-type Ca^{2+} channels can be effectively modulated by neurotransmitters and peptides through the activation of membrane receptors and coupled G proteins (for a review see Hille, 1994; Carbone et al., 1996). Receptor activation causes strong inhibitions of Ca^{2+} currents at low membrane potentials (−20 to 0 mV) that are effectively removed at higher voltages. Removal of inhibition is voltage-dependent (V-dependent) and is revealed by marked prolongations of Ca^{2+} channel activation at low potentials (Marchetti et al., 1986; Bean, 1989) and quick recruitments of Ca^{2+} currents (facilitation) after strong membrane depolarizations (Grassi and Lux, 1989; Elmslie et al., 1990). Many groups agree that most of the V-dependent inhibition and facilitation of Ca^{2+} channels is due to changes of channel gating activation (Grassi and Lux, 1989; Elmslie et al., 1990; Lopez and Brown, 1991; Kasai, 1992; Pollo et al., 1992; Boland and Bean, 1993; Golard and Siegelbaum, 1993) induced by direct interactions of pertussis toxin-sensitive G proteins with resting Ca^{2+} channels (Dolphin, 1991; Diversé-Pierluissi et al., 1995). There are, however, alternative explanations to this view. For instance, Ca^{2+} current depression by neurotransmitters may derive from a partial decrease of Ca^{2+} channel permeability due to interactions of activated G proteins with the ion-binding sites inside the pore and responsible for Ca^{2+} ion permeation (Kuo and Bean, 1993). In addition, single-channel data support the idea that Ca^{2+} channel inhibition by neurotransmitters favors the slow transition of Ca^{2+} channel gating from modes of high open probability to modes of low open probability, with little or no evidence for a V-dependent facilitation or delayed channel openings (Delcour and Tsien, 1993). These findings and those of Meriney et al. (1994), showing that slowdown of Ca^{2+} current activation may be weak in intact cells, argue against a significant role of V-dependent modulation in cell-attached patches in favor of V-independent mechanisms that down-modulate Ca^{2+} channels without affecting their activation kinetics (Luebke and Dunlap, 1994).

Here we show that inhibition of single N-type channels in IMR32 cells by noradrenaline and δ-opioid agonists is due primarily to the delay of first channel openings and only partially to a decreased open probability. In agreement with others (Lipscombe et al., 1989; Shen and Surprenant, 1991; Toselli and Taglietti, 1994) the single N-type channel conductance is not affected by the presence of receptor agonists. Prolongation of the first latency in cell-attached patches accounts nicely for both the kinetics slowing during test depolarization and for the current facilitation after pre-pulses in whole-cell recordings of IMR32 cells (Pollo et al., 1992), proving that kinetic slowings of N-type currents can also be revealed in intact cells (but see Meriney et al., 1994). Using a Monte Carlo routine to generate single-channel activity, our findings could be simulated by kinetic models predicting long latencies of transmitter-modified channels while preserving the channel conductance and the mean open time (Grassi and Lux, 1989; Elmslie et al., 1990;

Received for publication 24 October 1995 and in final form 31 January 1996.

Address reprint requests to Dr. Emilio Carbone, Dipartimento di Neuroscienze, Corso Raffaello 30, I-10125 Torino, Italy. Tel.: 39-11-6707786; Fax: 39-11-6707708; E-mail: carbone@unito.it.

0006-3495/96/05/2144/11 $2.00

Lopez and Brown, 1991; Kasai, 1992; Pollo et al., 1992; Boland and Bean, 1993).

A preliminary account of these findings has already appeared in abstract form (Carbone et al., 1995) in concomitance with the presentation of similar data on the N-type channel of frog sympathetic neurons (Elmslie and Kelly, 1995).

MATERIALS AND METHODS

Cell culture and solutions

IMR32 human neuroblastoma cells were grown in culture as previously described (Carbone et al., 1990) and used 7–12 days after differentiation. The culture medium contained Dulbecco's minimum essential medium supplemented with 10% heat-inactivated calf serum, penicillin (100 IU/ml), streptomycin (100 μg/ml), and L-glutamine (2 mM).

In cell-attached experiments the bathing solution contained (in mM): 135 potassium aspartate, 1 $MgCl_2$, 10 HEPES (pH 7.3 with KOH), and 5 EGTA to zero the resting membrane potential. The control pipette filling solution contained (in mM): 100 $BaCl_2$, 10 tetraethylammonium chloride (TEACl), 1 $MgCl_2$, 10 HEPES (pH 7.3 with TEAOH), and 300 nM tetrodotoxin (TTX). In whole-cell clamp experiments with high and low external [Ba^{2+}] the bath contained (in mM) either 100 $BaCl_2$, 10 TEACl, 1 $MgCl_2$, 10 HEPES (pH 7.3 with NaOH), and 300 nM TTX, or 10 $BaCl_2$, 125 NaCl, 1 $MgCl_2$, 10 HEPES, and 300 nM TTX. The internal perfusion solution was (in mM): 110 CsCl, 30 TEACl, 10 EGTA, 1 $MgCl_2$, 10 HEPES (pH 7.3 with CsOH), 2 ATP, and 0.25 cAMP. Noradrenaline (NA) (Sigma Chemical Co., St. Louis, MO) was weekly prepared in 1 mM stock solutions, light protected, and stored at 4°C. D-Pen_2-D-Pen_5-enkephalin (DPDPE) (Sigma Chemical Co.) was frozen in 1 mM stock solutions and light protected. Both agonists were dissolved daily to the final concentrations, either in the bath solution during whole-cell clamp measurements or in the pipette filling solution during cell-attached recordings. Nifedipine (Bayer AG, Wuppertal, Germany) was prepared as 1 mM stock solutions in 100% ethanol and stored light-protected at 4°C. The drug was dissolved at 5 μM final concentration in bath solutions as well as in the cell-attached pipette filling solution. The perfusion system consisted of a multi-barreled glass pipette held close to the cell (Carbone and Lux, 1987).

Current recordings and data acquisition

Patch electrodes were fabricated from thick borosilicated glasses (Hilgenberg, Malsfeld, Germany). For cell-attached recordings the electrode capacitance was further reduced by coating the pipette with Sylgard 184 (Dow Corning Corp., Midland, MI) (Magnelli et al., 1996). The final pipette resistance ranged between 7 and 9 MΩ for cell-attached recordings and 3 to 5 MΩ for whole-cell recordings. Junction potentials were between 3 and 4 mV and were not corrected, because the ionic content of the pipette and bath solutions remained unchanged during experiments.

Whole-cell currents and single-channel activity in the cell-attached patch configuration were recorded with a List EPC-7 amplifier (List Electronic, Darmstadt, Germany) through a 50-GΩ feedback resistor (Hamill et al., 1981). Current traces were acquired at digitizing rates of 5 to 10 kHz and filtered to 2 kHz with an 8-pole low-pass Bessel filter. Membrane stimulation and data acquisition were performed by using pClamp software (Axon Instrument, Foster City, CA) and a 12-bit A/D Tecmar Lab Master board (125 kHz) interfaced with an Intel 486-based computer. Voltage steps or ramp commands of 100 to 200 ms duration and variable amplitude were delivered at intervals of 5 to 10 s, both to limit the rundown of Ca^{2+} channels and to allow their recovery from inactivation. The holding potential was −90 mV.

Fast capacitative transients were minimized on line by the patch-amplifier setting. During single-channel recordings the residual capacitative and leak currents were corrected off-line by subtracting an average of sweeps with no channel activity (nulls). In whole-cell clamp measurements the capacitative current was minimized by subtracting the Cd^{2+}-insensitive currents remaining after the addition of 200 μM $CdCl_2$. All of the experiments were performed at room temperature (20–22°C).

Single-channel analysis

Unitary events were analyzed using AutesP software (Garching Innovation, Munich, Germany). Channel openings were detected by the half-amplitude criterion (Colquhoun and Sigworth, 1995) and converted into idealized events by means of interactive fitting routines (Carbone and Lux, 1987). Open and closed duration were measured on idealized records by setting the minimum resolvable duration to 200–300 μs. Fits of amplitude histograms, open and closed time distribution, were performed with the maximum-likelihood algorithm using a Simplex routine (Colquhoun and Sigworth, 1995). First latency histograms were constructed by calculating the time laps between the onset of the step depolarization and the first channel opening (Brown et al., 1984). Because of the limited number of events per patch, histograms were constructed by pooling data from a variable number of patches. Only patches containing one channel were taken into account. For each sweep the open probability (p_o) was calculated as $p_o = t_o/(t_o + t_c)$, where t_o and t_c represent the total time the channel spent in the open and closed states, excluding the first and last closures during the depolarization (Colquhoun and Sigworth, 1995; Delcour et al., 1993). This allows a more accurate estimate of p_o in current traces exhibiting a marked time-dependent inactivation of channel activity. Activation curves, $p_o(V)$, were obtained by averaging the p_o values at a given voltage over a number of sweeps (Magnelli et al., 1996).

The channel conductance and the corresponding single-channel current-voltage relationship (I/V) were estimated by measuring the open-channel amplitude at potentials ranging between −10 and +40 mV. At higher depolarizations the channel amplitude was too small (<0.6 pA) to be resolved from the background noise, whereas at lower depolarizations the probability of opening was too low to obtain a sufficient number of events. Unitary events of small amplitude (<0.5 pA at +20 mV) were occasionally observed but were not included in the analysis. Ensemble currents were obtained by averaging a variable number of sweeps. All data are given as mean ± SEM for n number of observations. Statistical significance (p) was calculated using Student's t-test.

RESULTS

Whole-cell current inhibition by NA and DPDPE in 10 and 100 mM [Ba^{2+}]

Single Ca^{2+} channel activity is usually recorded in high Ba^{2+} solutions (100 mM). With respect to whole-cell recordings in 10 mM Ba^{2+}, single-channel activity is thus expected to be shifted by +30 mV (Elmslie et al., 1994) and less depressed by neurotransmitters (Kuo and Bean, 1993). To verify this, we first compared the action of noradrenaline (NA) and δ-opioid agonists on macroscopic currents in 10 and 100 mM Ba^{2+}. NA (10 μM) and the δ-selective agonist DPDPE (1 μM) had similar action on IMR32 cells in 10 mM Ba^{2+} (Fig. 1, A_1 and A_2). The current depression by the two agonists was accompanied by a prolongation of Ca^{2+} channel activation and was largely relieved above +50 mV (Fig. 1, A_3 and A_4). The action of NA was mediated by α_2-adrenergic receptors (Pollo et al., 1992), and that of DPDPE was prevented by the unselective opioid antagonist naloxone (Fig. 1 A_2). Neither agonist exhibited action on low-voltage-activated currents (LVA) (*arrows* in Fig. 1, A_3 and A_4), and thus they were selective for the N-type channel

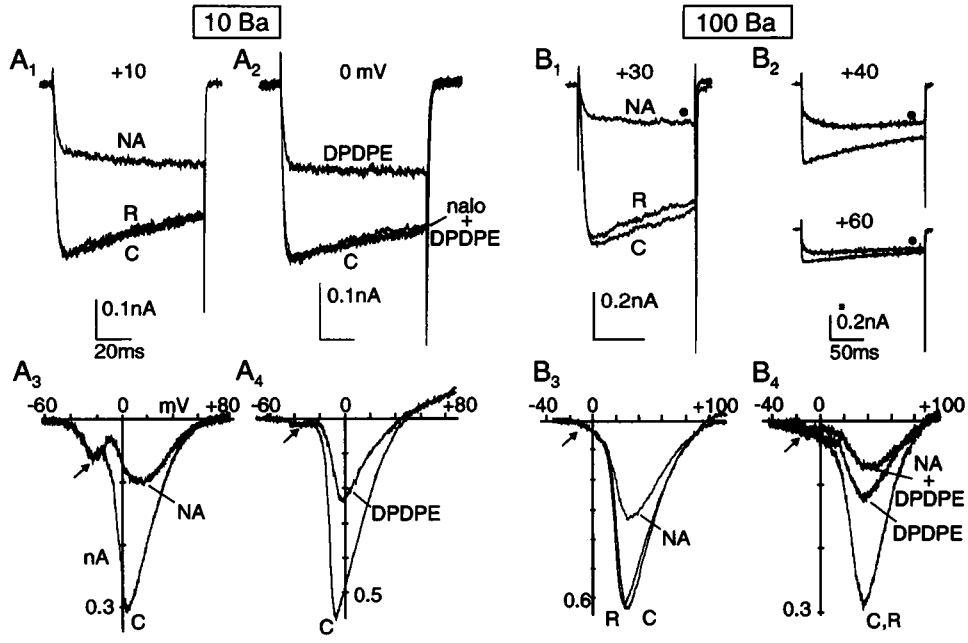

FIGURE 1 Inhibition of whole-cell Ba^{2+} currents by NA and DPDPE in 10 and 100 mM [Ba^{2+}]. (*A*) Effects of NA (10 μM) and DPDPE (1 μM) on high-voltage-activated (HVA) currents in 10 mM external Ba^{2+} at the potentials indicated. In A_1 the current traces were recorded at +10 mV before (C) and during (NA) NA application and after washing (R) from −90 mV holding potential. In A_2 the control trace (C) was recorded before application of the δ-agonist (DPDPE). Addition of the nonspecific opioid antagonist naloxone prevented the action of DPDPE (nalo + DPDPE). (A_3, A_4) *I/V* curves recorded in response to ramp commands with a slope of 0.55 mV/ms from −90 mV holding potential, before (C) and during application of NA (10 μM) or DPDPE (1 μM) in 10 mM Ba^{2+}. In A_3 the resulting *I/V* relationships show an early peak at around −25 mV (LVA, *arrow*) that is unaffected by NA and a second peak at about +4 mV (HVA) that is largely depressed by the transmitter. In A_4 the LVA current (*arrow*) is less evident, whereas the HVA component peaks at −9 mV, i.e., at slightly more negative potentials than in A_3. (*B*) Effects of NA and DPDPE on whole-cell Ba^{2+} currents in 100 mM external Ba^{2+}. (B_1) Reversible effects of NA (20 μM, ●) on HVA Ba^{2+} currents at +30 mV. (B_2) NA causes a marked slowdown of HVA channel activation at +40 mV (*top panel*, ●) that is accelerated at +60 mV (*bottom panel*). (B_3, B_4) *I/V* curves recorded in response to ramp commands similar to *A*, before (C) and during application of NA (20 μM) or DPDPE (1 μM) and after washing (R). In B_4 application of NA + DPDPE caused a greater inhibition of DPDPE alone. Trace C is the average current recorded before and after application of DPDPE alone and DPDPE + NA. V_h, −90 mV.

that is the predominant high-voltage-activated (HVA) channel in IMR32 cells (Carbone et al., 1990; Fox, 1995).

NA and DPDPE preserved their inhibitory effects in high Ba^{2+} solutions containing 5 μM nifedipine to block L-type channels (Fig. 1 *B*). In 100 mM Ba^{2+}, the N-type channel activated above 0 mV and reached maximum amplitudes between +29 and +46 mV (mean +39 ± 2 mV, n = 10), i.e., at about 35 mV more positive potentials with respect to 10 mM Ba^{2+}. In high Ba^{2+}, NA and DPDPE had almost no effect on the *I/V* curve region corresponding to the activation of low-threshold channels (*arrows* in Fig. 1, B_3 and B_4) but, in contrast, exerted marked inhibition on the dominant part of the *I/V* curve associated with the N-type channel. In 10 cells bathed in 100 mM Ba^{2+}, NA inhibition at +20 mV was 61 ± 3%. Compared with the 65% maximum inhibition in 10 mM Ba^{2+} (Pollo et al., 1992), this suggests a partial but not drastic reduction of neurotransmitter effects on N-type channels in high Ba^{2+} solutions (Kuo and Bean, 1993). NA action was also markedly V-dependent. The slower kinetics of Ba^{2+} currents was easily visible below +40 mV and speeded up at higher voltages (Fig. 1 B_2). DPDPE usually had smaller effects compared to those of NA alone, and the addition of DPDPE to NA caused either no additive action or a partial increased inhibition (Fig. 1 B_4).

Single N-type channels in IMR32 cell-attached patches

N-type channel activity was recorded in cell-attached patches with pipettes containing 100 mM Ba^{2+} and 5 μM nifedipine to block L-type channels. The activity of these channels was hardly visible at potentials below −10 mV from −90 mV holding potential (Fig. 2 A_1). Most traces showed either no or few short openings. At −10 mV, p_o was 0.05 and increased steeply with voltage (0.11 at 0 mV and 0.47 at +40 mV) (Fig. 2 *A*). Above 0 mV most traces showed channel activity. Some traces exhibited rapid open-closed events that were limited to the beginning of the pulse, whereas other traces showed no channel activity at all. The delay of first openings (first latency) decreased with voltage. At +10 mV the mean first latency was 11.4 ± 2 ms and decreased to 5.7 ± 1 ms at +20 mV. Traces above +20 mV started soon after the onset of step depolarizations and showed relatively few null sweeps. Amplitude histograms at potentials of high channel activity were well fitted by nar-

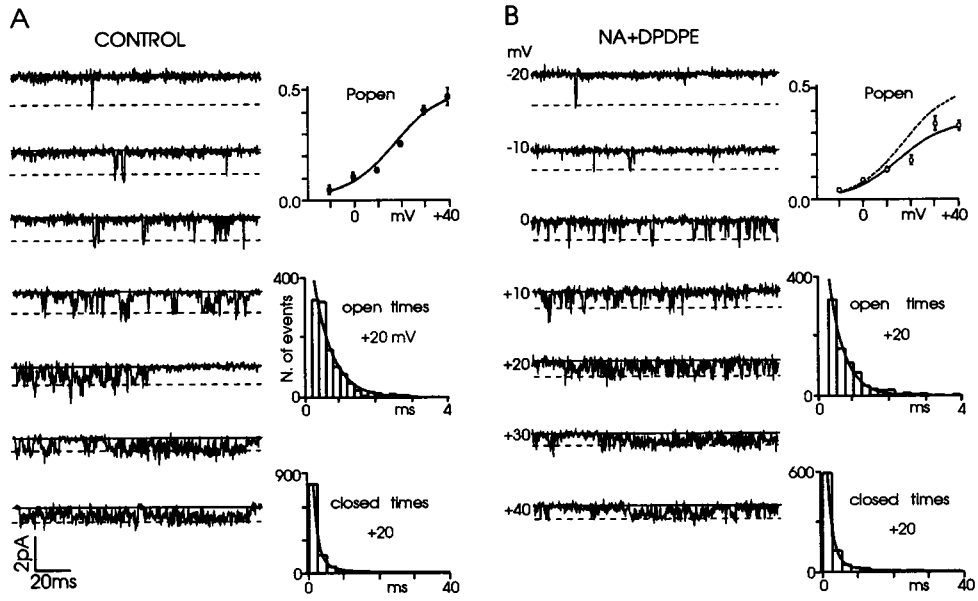

FIGURE 2 Single N-type channel recordings and their kinetic parameters in cell-attached patches at control (*A*) and with receptor agonists (*B*). The representative unitary N-type currents were recorded in control conditions (*A*) and with NA (20 μM) + DPDPE (1 μM) in the pipette (*B*) at the indicated potentials from $V_h = -90$ mV. Nifedipine (5 μM) was present inside and outside the pipette. (*Top diagrams*) Open probability of single N-type channels versus voltage. The data represent averages of p_o at different potentials from 10 patches in control conditions and 18 patches with NA + DPDPE, fitted by a Boltzman function: $p_o = p_{omax}\,(1 + \exp[(V_{½} - V)/k])^{-1}$ with $V_{½} = +22.9$ mV, $k = 12.9$ mV, $p_{omax} = 0.6$ (*solid curve* in *A*) and $V_{½} = +19.2$ mV, $k = 12.3$ mV, $p_{omax} = 0.4$ (*solid curve* in *B*). The dashed curve in *B* is taken from *A*. (*Middle diagrams*) Open time distributions at +20 mV. The curves are single exponential function with $\tau_o = 0.59$ ms (*A*) and 0.49 ms (*B*), respectively. (*Bottom diagrams*) Closed time distributions at control and with the two agonists in the pipette at +20 mV. The curves are double exponential functions with $\tau_{c1} = 1.25$ ms, $\tau_{c2} = 5.37$ ms (*A*), and $\tau_{c1} = 1.49$ ms, $\tau_{c2} = 5.74$ ms (*B*).

row Gaussian distributions (mean -0.9 ± 0.2 pA at +20 mV) (not shown). Between -20 and +40 mV the mean elementary current gave linear *I/V* relationships with a slope conductance of 19.0 ± 0.1 pS (*solid line* in Fig. 3 *A*). Open and closed time histograms were fitted with single and double exponential functions, respectively. At +20 mV the mean open time (τ_o) was 0.59 ms (Fig. 2 *A*) and increased weakly from +10 to +30 mV (*filled dots* in Fig. 3 *B*). At the same potential, mean closed times (τ_{c1} and τ_{c2}) were 1.25 ms and 5.37 ms (Fig. 2 A) and decreased steeply with increasing voltages (*filled dots* in Fig. 3, *C* and *D*). These values suggest a nice correspondence between the N-type channel of IMR32 cells and that of rat sympathetic neurons (Plummer et al., 1989): γ (19 vs. 20.6 pS), τ_o (0.59 ms vs. 0.53 ms at +20 mV), and p_o (0.11, 0.41 vs. 0.12, 0.42 at +10 and +30 mV, respectively).

NA and DPDPE have weak action on p_o, τ_o, and τ_c

The inhibitory effects of neurotransmitters on single N-type channels were studied in cell-attached patches distinct from controls. To increase the probability of observing the inhibitory action of neurotransmitters on the same Ca^{2+} channel, NA and DPDPE were applied simultaneously. The effects of both agonists were similar to those of NA alone, except that they were observed more frequently (in 70% rather than in 50% of the patches). This is because, very likely, the presence of both agonists enhanced the probability of finding either activated α_2-adrenergic or δ-opioid receptors in the vicinity of a functional Ca^{2+} channel. NA (20 μM) and DPDPE (1 μM) had nearly no effects on the single-channel conductance and mean open time. The mean slope conductance was 19.2 ± 0.1 pS (*dashed line* in Fig. 3 *A*), and the open times distribution was well fitted by a single exponential function with a τ_o slightly smaller than control: 0.49 versus 0.59 ms at +20 mV (Fig. 2 *B*). There was no clear indication of double exponential distributions of open times in the potential range examined, and τ_o preserved a weak voltage dependency similar to that in control patches (*empty circles* in Fig. 3 *B*). The two agonists, on the contrary, reduced p_o significantly and partially increased the mean closed times. The decrease in p_o was evident above +20 mV (*empty circles* in Fig. 2 *B*), where channel activity was sufficiently high to determine p_o with accuracy. Below +20 mV the decrease in p_o was less evident, very likely because of the low number of events at these potentials that did not allow an accurate determination of p_o ($p < 0.15$). The increase in τ_{c1} and τ_{c2} with respect to control (*empty circles* in Fig. 3, *C* and *D*) is in line with the decrease in p_o and the reduced value of τ_o, suggesting that Ca^{2+} channel inhibition by neurotransmitters is partially due to an increased probability of the channel to stay closed.

Close inspection of the distribution function of p_o at different potentials suggested that the lowering of p_o induced by the two agonists is not followed by drastic changes in the shape of the histograms (Fig. 3, *E* and *F*). This would

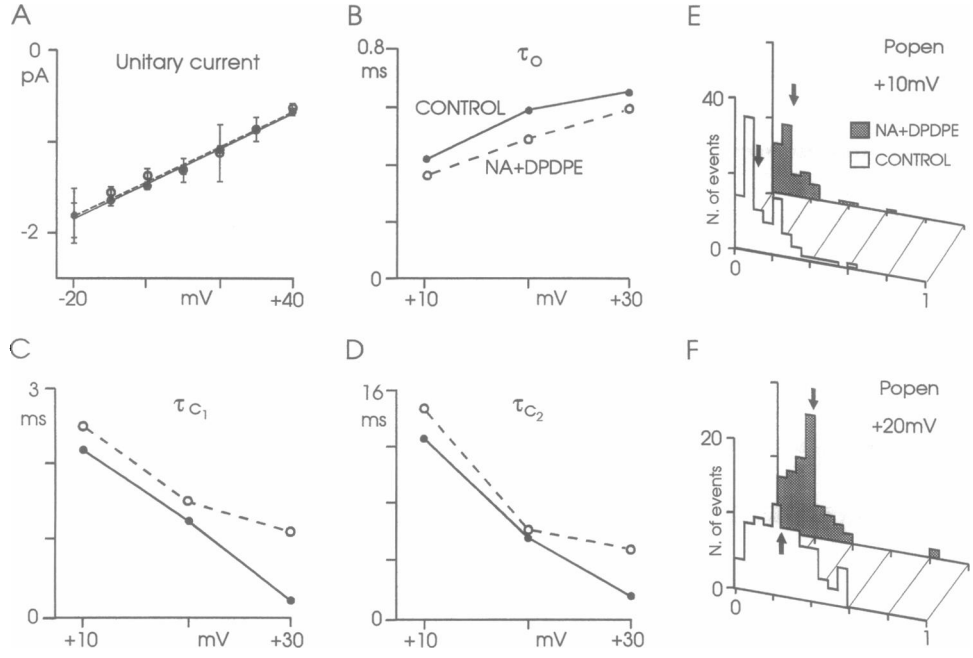

FIGURE 3 NA and DPDPE have little effect on single-channel conductance, kinetic parameters, and p_o distribution function. (*A*) Unitary *I/V* relationships of open N-type channels at control (*filled circles, solid line*) and with NA + DPDPE in the pipette (*empty circles, dashed line*). Data are mean values from $n = 10$ (control) and $n = 18$ patches (NA + DPDPE). The two regression lines have a mean slope conductance of 19 ± 0.1 pS and 19.2 ± 0.1 pS, respectively. (*B, C, D*) Mean open time τ_o and mean closed times τ_{c1} and τ_{c2} at control (●) and with NA + DPDPE in the pipette (○) are plotted versus voltage. Data were obtained from the exponential fit of the open and closed time distributions at +10, +20, and +30 mV, as illustrated in Fig. 2. (*E, F*) Open channel probability distributions at +10 and +20 mV in control conditions (*empty histogram*) and in the presence of NA + DPDPE (*shadowed histogram*). The mean p_o values indicated by the arrows are 0.13 (control) and 0.11 (NA + DPDPE) at +10 mV (*E*) and 0.25 and 0.19 at +20 mV (*F*).

be expected if the decrease in p_o was due to a shift from a high-p_o gating mode to a well-separated and long-lasting low-p_o mode (Delcour et al., 1993). At +10 and +20 mV, histograms at control and in the presence of the two agonists appeared to be more or less centered around their mean values (*arrows* in Fig. 3, *E* and *F*), showing no signs of second distributions with well-resolved relative maxima. The same occurred at +30 mV, where most of the p_o values were included between 0 and 0.8 at control and between 0 and 0.6 with NA + DPDPE (not shown). Thus, analysis of p_o distributions did not allow any clear distinction of multiple gating modes for the N-type channel in IMR32 cells, as reported for the Ca^{2+} channels of bullfrog sympathetic neurons (Delcour et al., 1993). This, however, does not necessarily imply that NA + DPDPE modified channels do not possess two gating modes with different mean p_o values. If the low-p_o mode, for instance, is short-lived and limited to the early part of the overall channel activity, then its contribution to the total p_o would be marginal. In this case, the p_o distribution function of modified channels would not deviate significantly from that of normal channels (see Discussion).

NA and DPDPE prolong the latency of first openings

The most remarkable effect of NA and DPDPE on Ca^{2+} channel activity was on both the mean latency of first openings and the number of null sweeps that increased from 35 to 55% at +20 mV. The control N-type channel activity that often started within a few milliseconds after the onset of the step depolarization was substantially delayed by the agonists, reaching maximum delays of 80 to 100 ms (Fig. 4). Channel activity occurred preferentially toward the end rather than at the beginning of the trace. The increased latency, however, varied largely from patch to patch. In a group of 12 cells showing remarkable activation delays, the mean latency at +20 mV was 24.9 ± 3.1 ms with NA + DPDPE, whereas channel activity in 12 control cells had mean latencies of 5.7 ± 1.0 ms ($p < 0.01$) (Fig. 4 *B*). In another group of seven cells showing marginal prolongations with NA + DPDPE, the mean latency increased to only 7.8 ± 1.6 ms.

Ensemble currents had very different time courses at control and with NA + DPDPE (*bottom traces* in Fig. 4 *A*). The control ensemble current activated rapidly and inactivated quickly and incompletely. The time to peak, t_p, was about 2 ms, and the time constant of inactivation (τ_{inact}) was 65.4 ms, whereas in the presence of the agonists, channel activation was slow and showed no sign of time-dependent inactivation. The agonist-modified current had rather a continuous rise that was best approximated with a double exponential function with $\tau_{fast} = 2.1$ ms and $\tau_{slow} = 24$ ms. Neurotransmitter inhibition at the peak of the control ensemble current was even larger than the percentage inhibition of macroscopic currents in 100 mM Ba^{2+} (65% vs.

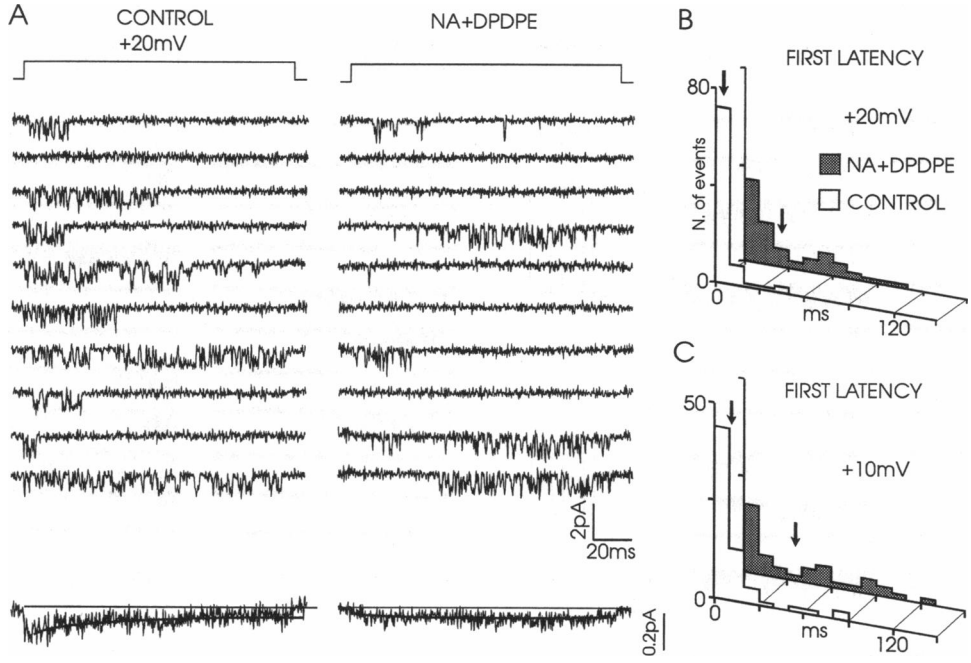

FIGURE 4 NA and DPDPE delay the first channel opening. (*A*) Single N-type channel traces recorded sequentially in a control patch (*left*) and with NA (20 μM) + DPDPE (1 μM) in the recording pipette (*right*) during depolarizations to +20 mV from V_h = −90 mV. Notice the prolonged delay of first openings and the increased number of null sweeps in the presence of the two agonists. Bottom traces represent the ensemble currents obtained by averaging 90 sweeps from 20 cells in control and 20 sweeps from one cell with NA + DPDPE. The control ensemble current (*bottom left*) was fast activating and partially inactivating, with a main decay time constant of 65.4 ms. The solid line through the noisy trace represents a double exponential function with time constants τ_1 = 8.1 ms (0.24), τ_2 = 65.4 ms (0.76) and normalized amplitudes in parentheses. The agonist-modified ensemble current (*bottom right*) was slowly activating and fitted by a double exponential function (*solid curve*) with τ_{fast} = 2.1 ms (0.12) and τ_{slow} = 24 ms (0.88). (*B*) First latency distributions at control (*empty diagram*) and with NA + DPDPE (*shadowed diagram*) derived from the same number of sweeps of the ensemble currents in *A*. The mean latencies indicated by the arrows were 5.7 ± 1.0 ms and 24.9 ± 3.1 ms, respectively. (*C*) Same as *B* but at + 10 mV. Mean latencies were 11.4 ± 2.0 ms at control and 35.8 ± 6.0 ms with NA + DPDPE.

61%). Thus, prolongation of the first latency and reduction of p_o account nicely for the amplitude depression and kinetics slowing of N-type channels by neurotransmitters. The same results were obtained at +10 mV. The mean latency in 22 control cells was 11.4 ± 2.0 ms and increased to 35.8 ± 6.0 ($p < 0.01$) in seven cells with pronounced latency in the presence of NA + DPDPE (Fig. 4 *C*).

Facilitation by pre-pulses restores N-type channel activation kinetics

The V-dependent inhibition of N-type channels by neurotransmitters can be quickly removed (facilitated) by strong depolarizations (Grassi and Lux, 1989; Elmslie et al., 1990). Pulses of 50 ms to potentials positive to +70 mV preceding a test depolarization to +20 mV are usually sufficient to recruit Ca^{2+} channels, which are inhibited by activated G proteins. The kinetic properties of the V-dependent inhibition and facilitation of single N-type channels were studied at +10 and +20 mV without and with a 40-ms conditioning pre-pulse to +120 mV. Pre-pulses of lower amplitude (+90 mV) and longer duration (100 ms) were equally effective. Sequential test depolarizations without and with pre-pulses were separated by 10-s intervals to limit channel run-down and allow recovery from inactivation. The protocol was repeated until channel activity disappeared. Fig. 5 shows a series of recordings of normal N-type channels during test depolarizations to +20 mV without (*left*) and with (*right*) the facilitating pre-pulse. Open probability and mean first latency remained nearly unchanged after the pre-pulse (*top* and *bottom diagrams*). Thus, like macroscopic Ba^{2+} currents, facilitatory pre-pulses did not alter drastically the size and the time course of control ensemble currents at the test potential (*bottom traces*). Open probability and mean first latency changed significantly after pre-pulses in the presence of NA + DPDPE. The delayed and reduced channel activity during a normal test at +20 mV (Fig. 6 *left*) was significantly accelerated and enhanced after the pre-pulse (*right*). p_o increased from 0.15 without to 0.21 with the pre-pulse ($p < 0.01$; *top diagram* in Fig. 6), and the mean latency decreased from 18.2 ms to 7.1 ms ($p < 0.01$, *bottom diagram*). Consistently, the time course of ensemble currents without and with the pre-pulse changed markedly. Ensemble currents were small and weakly inactivating without pre-pulse but about threefold larger and fast decaying after pre-pulse. The ensemble current decay was fitted with a single exponential with a 21.1-ms time constant of re-inhibition smaller than τ_{inact} in control conditions (41.3 ms before pre-pulse; *bottom trace* in Fig. 5 *left*). This suggests that, as for macroscopic Ba^{2+} currents, re-inhibition of

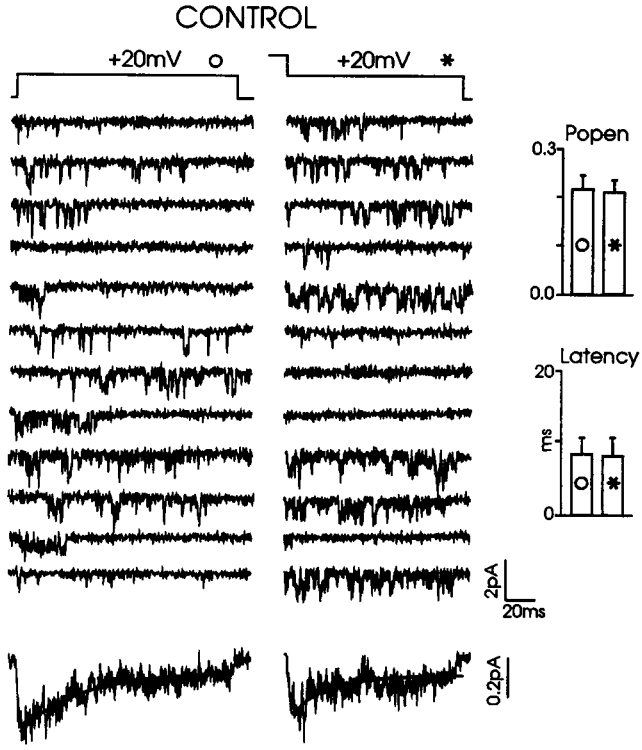

FIGURE 5 Single N-type channel activity in control conditions before and after conditioning pre-pulse. The unitary N-type channel currents were recorded at +20 mV before (*left column*) and after (*right column*) application of a 40 ms pre-pulse depolarization to +120 mV in control conditions. Recordings without and with the pre-pulse were repeated sequentially at intervals of 10 s. Notice the nearly unchanged single-channel activity, amplitude, and time course of ensemble currents (*bottom traces*). The ensemble currents on the bottom were obtained by averaging 33 sweeps. The solid curve fitting the ensemble current before pre-pulse is a double exponential with τ_{fast} = 21.4 ms (0.12) and τ_{slow} = 41.3 ms (0.88) and a single exponential after pre-pulse (τ = 25 ms). On the right are the mean p_o and mean first latency calculated before (○) and after (*) pre-pulse. Notice the mainly identical values of p_o and first latency with and without pre-pulse.

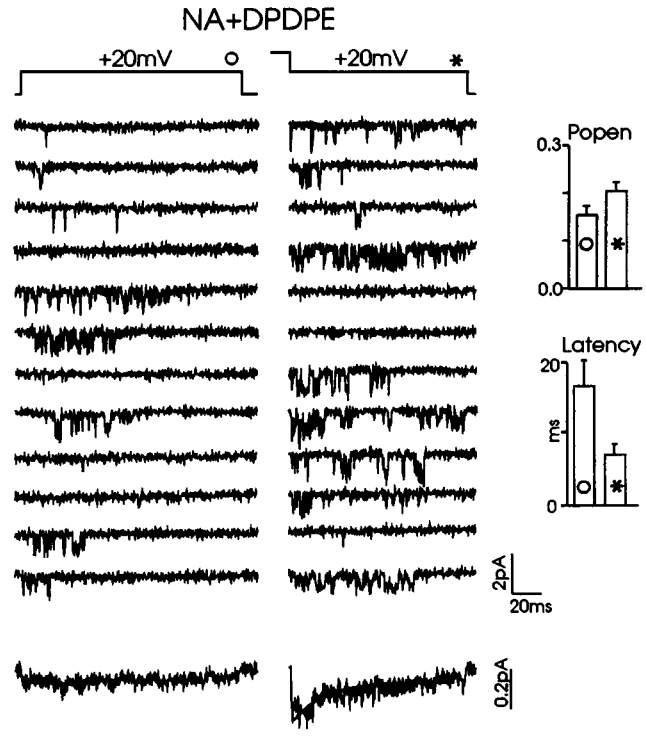

FIGURE 6 Facilitation of single N-type channel activity by pre-pulse in the presence of NA + DPDPE. Same conditions as in Fig. 5 but in the presence of NA (20 μM) and DPDPE (1 μM) in the pipette. In most traces the delayed openings induced by the two agonists (*left column*) were accelerated by the pre-pulse to +120 mV (*right column*). There were, however, exceptions to this rule. For instance, the channel activity of trace 3 remained unchanged and that of trace 5 and 6 was depressed by the pre-pulse. The time course and size of ensemble currents was markedly different before and after pre-pulses (*bottom traces*). The rising phase of the current before pre-pulse was fitted with a double exponential with τ_{fast} = 1.1 ms (0.72) and τ_{slow} = 17.8 ms (0.28), whereas the current decay after pre-pulse was fitted by a single exponential (τ = 21.1 ms). Ensemble currents were obtained by averaging 54 traces. On the right are the mean p_o and mean first latency calculated before (○) and after (*) pre-pulse. Notice the increase of p_o and the marked decrease of the first latency after pre-pulse.

facilitated channels may occur at a faster rate than channel inactivation (Lopez and Brown, 1991; Pollo et al., 1992; Kasai, 1992). Similar findings were obtained with test potentials to +10 mV. In control conditions the mean p_o and first latency before and after pre-pulse were comparable, whereas with NA + DPDPE, p_o increased from 0.08 to 0.12 and first latency decreased from 28 to 12 ms.

V-independent inhibition of single N-type channels

Pre-pulses were not always effective in removing NA + DPDPE inhibition. In most patches the conditioning pre-pulse was unable to facilitate the modified channel activity in 12% of the traces and induced steady inactivation in another 10%. In the first case, the low p_o and the prolonged first latencies in the presence of the agonists remained unchanged after pre-pulse, as expected if neurotransmitter inhibition was predominantly V-independent during that epoch (*trace 3* in Fig. 6). This would correspond to the Ca^{2+} channel modulation in which whole-cell currents are mainly depressed without changing their activation time course (Delcour and Tsien, 1993). In the second case, channel activity was little affected by the agonists and strongly inactivated by the pre-pulse (*traces 5* and *6* in Fig. 6 and *traces 7* and *8* in Fig. 5). This action was also often observed in control conditions and was attributed to long sojourns of the channel in its inactivated state or to V-dependent inactivation during strong depolarizations.

DISCUSSION

An extensive literature based on macroscopic current recordings suggests that Ca^{2+} current depression by neurotransmitters derives from a membrane-delimited coupling between receptor-activated G proteins and high-threshold

Ca^{2+} channels (for a review see Swandulla et al., 1991; Tsien et al., 1991). Ca^{2+} channel inhibition is partially removed with increasing voltages, causing both a pronounced slowdown of Ca^{2+} current activation during test depolarizations (Marchetti et al., 1986; Bean, 1989) and a massive recruitment (facilitation) of Ca^{2+} channel after large pre-pulses (Grassi and Lux, 1989; Elmslie et al., 1990). These effects are common to most neurons, involve a variety of membrane receptors, and are selective for non-L-type high-threshold Ca^{2+} channels (N- and P/Q-type). Our data on the single N-type channel of IMR32 cells fit this concept nicely and suggest that slowdown of Ca^{2+} channel activation by receptor agonists is mostly due to well-resolved transitions of Ca^{2+} channels from a modified to a normal gating condition. Modified channels open with some delay at potentials of half-maximum activation (+20 mV in 100 mM Ba^{2+}) and can be effectively accelerated (facilitated) by conditioning pre-pulses to give large ensemble currents that quickly decay to their inhibited level. Thus, single N-type channels of IMR32 cells possess all of the kinetic prerequisites to mimic the V-dependent inhibition of neuronal Ca^{2+} currents by neurotransmitters.

V-dependent modulation viewed through single-channel recordings

Figs. 4 and 6 show clearly that N-type channels open with long delays when affected by neurotransmitters. First latency is prolonged fivefold and channel activity is largely recovered after this delay; p_o is 35% smaller than control at +20 mV but differs by only 20% at +30 mV. This corresponds reasonably well to the V-dependent removal of neurotransmitter inhibition on macroscopic currents. The time constant of current activation is prolonged from 2 ms (τ_{fast}) to 15–30 ms (τ_{slow}), and the size of the current gradually recovers with increasing voltages (Marchetti et al., 1986; Bean, 1989). Indeed, the correspondence between the prolongation of macroscopic currents and the first latency increase of unitary currents could be even closer if some of the null sweeps recorded with the agonists would have been interpreted as missed long latencies and included in the determination of mean first latencies (Fig. 4 *B*). We found in all cases a nice correspondence between the time courses of ensemble and macroscopic currents. Control ensemble currents activate with times to peak comparable to macroscopic currents (~2 ms at +20 mV), whereas modified ensemble currents turn on with long delays and hardly reach a steady-state value during pulses of 150 ms. Similar effects are also shown for the muscarinic inhibition of HVA channels in outside-out patches of rat hippocampal neurons (Toselli and Taglietti, 1994).

The voltage dependency of Ca^{2+} channel modulation by neurotransmitters is best proved by Ca^{2+} channel recruitment using conditioning pre-pulses (Grassi and Lux, 1989; Elmslie et al., 1990). Small and slowly rising currents recover their fast activation and large amplitude after strong pre-pulses. The same thing occurs at the single-channel level. The low-p_o and long latency of modified channels return to nearly control values (high-p_o and short latency) after brief and large depolarizations. Facilitated channels, which are open after the pre-pulse, give rise to a rapidly decaying current that approaches a steady-state value toward the end of the test pulse. This current relaxation reflects the time course of channel re-inhibition after facilitation (τ_{reinh} = 20 to 30 ms) (Lopez and Brown, 1991; Kasai, 1992), which is faster than but not easily separable from channel inactivation (τ_{inact} = 30–60 ms). Facilitation and fast re-inhibition of single Ca^{2+} channels on return to +30 mV has also recently been reported for the N-type channel of frog sympathetic neurons in the presence of NA (Elmslie and Kelly, 1995).

V-independent modulation of single Ca^{2+} channels

Neurotransmitter inhibition cannot be fully recovered by strong depolarizations (Formenti et al., 1993; Luebke and Dunlap, 1994). About 20–30% of the total current may be persistently inhibited by neurotransmitters even after strong depolarizations. This also occurs at the single-channel level. Most patches with marked V-dependent features (low p_o and prolonged latencies) also showed a small percentage of traces with low p_o that were not recovered by pre-pulses. These traces obviously contribute little to the total current before and after pre-pulse, lowering the degree of V-dependent facilitation. Thus, single-channel recordings support the presence of a moderate V-independent inhibition of N-type channel in IMR32 cells in combination with a predominant V-dependent action. If, as proposed (Diversé-Pierluissi et al., 1995), the voltage dependence and voltage independence of Ca^{2+} channel modulation are mediated by distinct G proteins, the higher probability of finding delayed channel openings in IMR32 cells indicates a microscopic predominance around the channel of G_o and G_i proteins responsible for the V-dependent inhibition. This implies also that Ca^{2+} channel modulation by neurotransmitters is a highly localized signal transduction mechanism in which the same channel may closely interact with a pool of distinct receptor-activated G proteins.

A persistent inhibition of channel activity with little sign of time-dependent removal during prolonged depolarizations is the primary action of NA in bullfrog sympathetic neurons (Delcour and Tsien, 1993). In patches exposed to 100 μM NA the N-type channel gating is shifted from a normal gating mode with high p_o to a modified gating mode with low p_o (Delcour et al., 1993). Modified channels, however, exhibit long sojourns (~10 s) in the low-p_o mode, making the transitions from low to high p_o rather unlikely throughout intervals of 200 ms. This originates NA-modified ensemble currents of smaller size but with a time course similar to that of control currents, which is at variance with most of our

present recordings and with the marked kinetic slowing of N-type channels by NA on the same cells (Elmslie and Kelly, 1995). A reason for this discrepancy may be that most of the single-channel activity recorded by Delcour and Tsien at −10 mV belongs to a non-N-type Ca^{2+} channel that activates at low voltages (−30, −10 mV in 110 mM Ba^{2+}) and is preferentially depressed by NA in a V-independent manner (Elmslie et al., 1994).

Effects of high $[Ba^{2+}]_o$ and cell dialysis on Ca^{2+} channel modulation

Consistent with previous reports (Delcour and Tsien, 1993; Toselli and Taglietti, 1994), NA + DPDPE does not significantly affect the single-channel conductance of N-type channels in IMR32 cells. This is at variance with the proposal of a reduction in the single-channel conductance by neurotransmitter-activated G proteins (Kuo and Bean, 1993). In this view, activated G proteins modify the arrangement of the charged groups inside the pore that are responsible for ion permeability (Kuo and Hess, 1993). The inhibition of the channel conductance by G proteins is favored at millimolar concentrations of Ba^{2+} ions (2–5 mM), whereas it is largely relieved at higher concentrations of permeating ions (100–150 mM). The mechanism predicts lowering of both the single-channel conductance and macroscopic Ba^{2+} currents in the presence of the neurotransmitter in low $[Ba^{2+}]_o$ solutions (~60% depression) and weaker inhibitions in high $[Ba^{2+}]_o$ solutions (~30%). We found, however, no visible reduction of the unitary events during intervals of low- and high-p_o activity, suggesting that high $[Ba^{2+}]_o$ solutions do not represent a serious limitation to revealing the V-dependent modulation of single Ca^{2+} channels.

Our findings also argue against the proposal that kinetic slowing of Ca^{2+} channels by neurotransmitters is not a consequence of the membrane-delimited coupling between activated G proteins and Ca^{2+} channel, but rather is due to the loss of some intracellular factor during internal cell dialysis (Meriney et al., 1994). Kinetic slowing is suggested to be an indirect effect of the whole-cell recording conditions rather than representing a true phenomenon belonging to intact cells. The present data show that in cell-attached patches of IMR32 cells the kinetic features of the V-dependent Ca^{2+} channel modulation are well preserved. The kinetic slowing parallels the V-dependent removal of inhibition and thus represents two aspects of the same phenomenon in both dialyzed and intact cells.

Model simulation of V-dependent inhibition and facilitation

Kinetic models based on macroscopic current measurements assume that V-dependent Ca^{2+} channel modulation by receptor-activated G proteins is primarily determined by channel gating modifications. All proposed models agree that channels shift from a normal (willing) to a modified (reluctant) gating condition and that membrane voltage regulates the percentage of modified channels that convert to normal during step depolarizations. Transitions between modified and normal channels are expected to occur during pulses of 100–200 ms at moderate voltages. We therefore tested whether a modified version of our model (Pollo et al., 1992) was able to simulate the present data. Simulation was achieved by describing the open-closed kinetics of Ca^{2+} channels in terms of a Markov chain of n channel states using the algorithm described by Colquhoun and Hawkes (1995). Transitions from one state to the next and a pattern of single-channel events were generated by a Monte Carlo routine (Rubinstein, 1981).

In the proposed model the Ca^{2+} channel possesses a normal and a modified gating mode. Each mode has two closed states (C_1, C_2 and C_1^*, C_2^*), one open state of equal conductance (O and O*), one inactivated state (I and I*), and different p_o values (high and low):

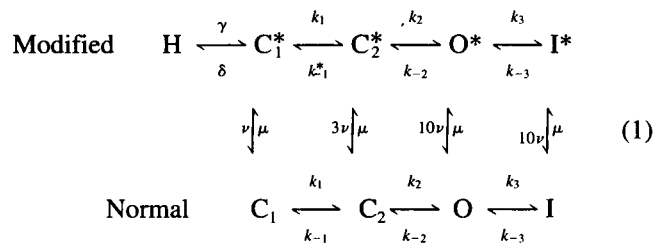

(1)

State H represents a modified closed state of the channel resulting from a reversible interaction with the G protein (Kasai, 1992; Pollo et al., 1992). The V-dependent rates γ, δ, and k^*_{-1} responsible for the slow activation and low p_o of modified channels were set low enough to mimic the long latencies of modulated channels. The activation rates k_1, k_{-1}, k_2, k_{-2} responsible for the fast activation and high p_o of normal channels were calculated from the experimental probability distribution function of the open and closed times at +20 mV (Brown et al., 1984). Transition $O^* \rightarrow C_2^*$ was assumed to be equal to $O \rightarrow C_2$ because the τ_o of modified channels was comparable to that of normal channels (Fig. 3 *B*). The inactivation rates (k_3 and k_{-3}) were set to reproduce the decaying time course of the normal ensemble current (Fig. 4).

Transitions between the two modes are regulated by the binding (μ) and unbinding (ν) of the activated G protein. The binding was assumed to occur independently of the state of the channel and to be fast at saturating concentrations of the agonists. The unbinding was assumed to increase 10-fold as the modified closed channels in C_1^* approach the open state O* (Elmslie et al., 1990; Boland and Bean, 1993). Under these conditions, most of the single-channel activity simulated by Scheme 1 derives from channels that during activation move (are facilitated) from the modified low-p_o mode to the normal high-p_o mode while only relatively few channels remain in the low-p_o mode and reach O*. This explains the apparent contradiction that despite the existence of two

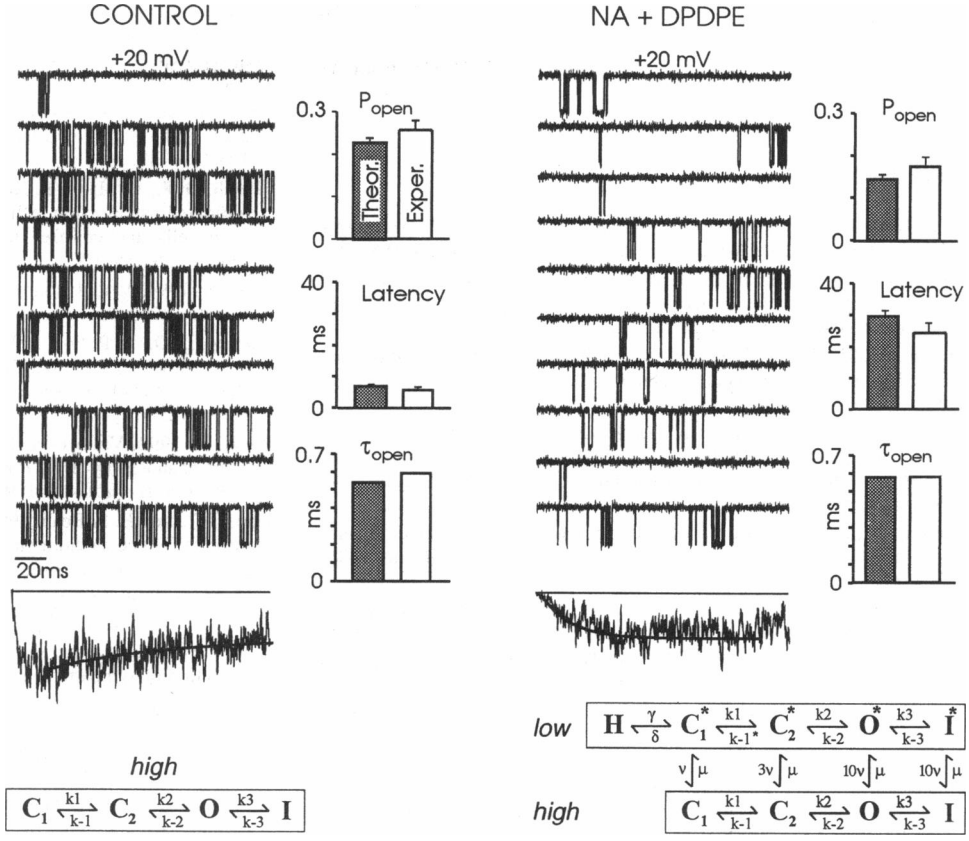

FIGURE 7 Monte Carlo simulation of single-channel activity and ensemble currents. Ten consecutive simulated traces at +20 mV are shown for control conditions (*left*) and in the presence of NA + DPDPE (*right*). An arbitrary white-noise signal was overlapped to the traces; the used schemes are indicated below each panel. Transition rates were set to (in ms^{-1}): k_1 = 0.22, k_{-1} = 0.09, k^*_{-1} = 0.45, k_2 = 0.68, k_{-2} = 1.69, k_3 = 0.015, k_{-3} = 0.0001, γ = 0.04, δ = 0.01, μ = 0.2, and ν = 0.01. At t = 0, the channel was assumed to occupy state C_1 under control conditions (*left*) or state H in the presence of NA + DPDPE (*right*). States H, C, C*, I, and I* were nonconductive, whereas states O and O* had equal conductance. The ensemble currents on the bottom are averages of 100 simulated traces and are fitted by single exponential functions with τ_{inact} = 69.7 ms (*left curve*) and τ_{slow} = 17.7 ms (*right curve*). Single-channel and ensemble current amplitudes are given in arbitrary scales. Block diagrams on each panel compare the p_o, first latencies, and τ_o of the simulated channel activity (*shadowed bars*) with the experimental values (*empty bars*).

gating modes with different p_o the distribution function of p_o with the agonists does not deviate significantly from the normal one (Fig. 3, *E* and *F*).

Single-channel events simulated by model 1 account for most of the kinetic features of neurotransmitter inhibition at +20 mV (Fig. 7). The simulated channel activates quickly at control (mean latency 6.8 ms) and flickers with mean open times (τ_o = 0.54 ms) and p_o (0.23) similar to those experimentally determined at the same potential (Figs. 2 and 5). In contrast, if the channel is in the modified gating mode the model produces an overall reduced activity with lower p_o values than control (0.14 vs. 0.23) but with a comparable mean open time (0.49 vs. 0.54) (Figs. 2 and 6). First latencies are markedly prolonged during the 160-ms time interval (30 ms vs. 6.8 ms), after which channel activity is partially recovered. Ensemble currents calculated from the simulated traces also exhibit close similarities to the experimental recordings (*bottom traces* in Fig. 4). τ_{inact} for control channels was 69.7 ms (vs. 65.4 ms in Fig. 4), and τ_{slow} of activation of modified currents was 17.7 ms (vs. 24.0 ms and 21.1 ms in Figs. 4 and 6).

Attempts to simulate single-channel activity with other models were also successful. With proper modifications the model of Boland and Bean (1993) could simulate nicely the prolonged latency and the ensemble current depressions induced by neurotransmitters but was unable to account for the decreased p_o in the presence of the agonists. Most models, including our Scheme 1, do not account for the partial V-independent inhibition and are unable to simulate a sufficient number of traces with no events. This is because "null" sweeps may represent inactivation from closed states, whereas most models assume that the channel must open before it inactivates. Null sweeps, however, contribute mainly to the overall current depression and do not significantly alter the slowing of channel activation.

CONCLUSIONS

We have shown that V-dependent Ca^{2+} channel modulation by neurotransmitters is well resolved in single-channel recordings of neuron-like cells expressing a majority of N-type channels (Carbone et al., 1990) and a sufficient density of noradrenergic and opioid receptors. Although dominant, the V-dependent modulation of the single Ca^{2+} channel coexists with a V-independent inhibition. The two phenomena appear to be neither limited by high Ba^{2+} concentration nor affected by cell perfusion. Given the importance of Ca^{2+} channel modulation for the autocrine control of neurotransmitters and hormone secretion (Hirning et al., 1988), our data reinforce the view that V-dependent Ca^{2+} channel modulation by neurotransmitters is a highly localized system with fast on-off kinetics (5–20 ms) that may help to quickly recruit a large number of Ca^{2+} channels, thus potentiating Ca^{2+} influx during cell activity.

This paper is dedicated to the late Hans Dieter Lux, who stimulated and encouraged this project.

Supported by NATO (grant CRG 0576/87 to EC) and by Telethon-Italy (grant 627).

REFERENCES

Bean, B. P. 1989. Neurotransmitter inhibition of neuronal calcium currents by changes in channel voltage-dependence. *Nature.* 340:153–156.

Boland, L., and B. P. Bean. 1993. Modulation of N-type calcium channels in bullfrog sympathetic neurons by luteinizing hormone-releasing hormone: kinetics and voltage-dependence. *J. Neurosci.* 13:516–533.

Brown, A. M., H. D. Lux, and D. L. Wilson. 1984. Activation and inactivation of single calcium channels in snail neurons. *J. Gen Physiol.* 83:751–769.

Carbone, E., V. Carabelli, M. Lovallo, H. Zucker, and V. Magnelli. 1995. Voltage-dependent inhibition and facilitation of single N-type channel kinetics by noradrenaline and δ-opioid agonists in IMR32 cells. *Soc. Neurosci. Abstr.* 21:514.

Carbone, E., and H. D. Lux. 1987. Single low-voltage-activated calcium channels in chick and rat sensory neurons. *J. Physiol. (Lond.).* 386: 571–601.

Carbone, E., V. Magnelli, A. Pollo, V. Carabelli, A. Albillos, and H. Zucker. 1996. Biophysics of voltage-dependent Ca^{2+} channels: gating kinetics and their modulation. *In* Ion Channel Pharmacology. B. Soria and V. Ceña, editors. Oxford University Press, Oxford. In press.

Carbone, E., E. Sher, and F. Clementi. 1990. Ca currents in human neuroblastoma IMR32 cells: kinetics, permeability and pharmacology. *Pflügers Arch. Eur. J. Physiol.* 416:170–179.

Colquhoun, D., and A. G. Hawkes. 1995. A Q-matrix cookbook. How to write only one program to calculate the single-channel and macroscopic prediction for any kinetic mechanism. *In* Single-Channel Recording, 2nd ed. B. Sakmann and E. Neher, editors. Plenum Press, New-York. 589–633.

Colquhoun, D., and F. J. Sigworth. 1995. Fitting and statistical analysis of single-channel records. *In* Single-Channel Recording, 2nd ed. B. Sakmann and E. Neher, editors. Plenum Press, New York. 483–587.

Delcour, A. H., D. Lipscombe, and R. W. Tsien. 1993. Multiple gating modes of N-type Ca^{2+} channel activity distinguished by differences in gating kinetics. *J. Neurosci.* 13:181–194.

Delcour, A. H., and R. W. Tsien. 1993. Altered prevalence of gating modes in neurotransmitter inhibition of N-type calcium channels. *Science.* 259:980–984.

Diversé-Pierluissi, M., P. K. Goldsmith, and K. Dunlap. 1995. Transmitter-mediated inhibition of N-type calcium channels in sensory neurons involves multiple GTP-binding proteins and subunits. *Neuron.* 14:191–200.

Dolphin, A. C. 1991. Regulation of calcium channel activity by GTP binding protein and second messengers. *Biochim. Biophys. Acta.* 1091: 68–80.

Elmslie, K. S., P. J. Kammermeier, and S. W. Jones. 1994. Reevaluation of Ca^{2+} channel types and their modulation in bullfrog sympathetic neurons. *Neuron.* 13:217–228.

Elmslie, K. S., and E. Kelly. 1995. Norepinephrine modulation of single calcium channels in frog sympathetic neurons. *Soc. Neurosci. Abstr.* 21:515.

Elmslie, K. S., W. Zhou, and S. W. Jones. 1990. LHRH and GTP-γ-S modify calcium current activation in bullfrog sympathetic neurons. *Neuron.* 5:75–80.

Formenti, A., E. Arrigoni, and M. Mancia. 1993. Two distinct modulatory effects on calcium channels in adult rat sensory neurons. *Biophys. J.* 64:1029–1037.

Fox, J. 1995. Irreversible and reversible blockade of IMR32 calcium channel currents by synthetic MVIIA and iodinated MVIIC ω-conopeptides. *Pflügers Arch. Eur. J. Physiol.* 429:873–875

Golard, A., and S. A. Siegelbaum. 1993. Kinetic basis for the voltage-dependent inhibition of N-type calcium current by somatostatin and norepinephrine in chick sympathetic neurons. *J. Neurosci.* 13: 3884–3894.

Grassi, F., and H. D. Lux. 1989. Voltage-dependent GABA-induced modulation of calcium currents in chick sensory neurons. *Neurosci. Lett.* 105:113–119.

Hamill, O. P., A. Marty, E. Neher, B. Sakmann, and F. J. Sigworth. 1981. Improved patch-clamp techniques for high-resolution current recording from cells and cell-free membrane patches. *Pflügers Arch. Eur. J. Physiol.* 391:85–100.

Hille, B. 1994. Modulation of ion-channel function by G-protein-coupled receptors. *Trends Neurosci.* 17:531–536.

Hirning, L. D., A. P. Fox, E. W. McCleskey, B. M. Olivera, S. A. Thayer, R. J. Miller, and R. W. Tsien. 1988. Dominant role of N-type Ca^{2+} channels in evoked release of norepinephrine from sympathetic neurons. *Science.* 239:57–61.

Kasai, H. 1992. Voltage- and time-dependent inhibition of neuronal calcium channels by a GTP-binding protein in a mammalian cell line. *J. Physiol. (Lond.).* 448:189–209.

Kuo, C-C., and B. P. Bean. 1993. G-protein modulation of ion permeation through N-type calcium channels. *Nature.* 365:258–262.

Kuo, C-C., and P. Hess. 1993. Characterization of the high-affinity Ca^{2+} binding sites in the L-type Ca^{2+} channel pore in rat phaeochromocytoma cells. *J. Physiol. (Lond.).* 466:657–682.

Lipscombe, D., S. Kongsamut, and R. W. Tsien. 1989. α-Adrenergic inhibition of sympathetic neurotransmitter release mediated by modulation of N-type calcium-channel gating. *Nature.* 340:639–642.

Lopez, H. S., and A. M. Brown. 1991. Correlation between G protein activation and reblocking kinetics of Ca^{2+} channel current in rat sensory neurons. *Neuron.* 7:1061–1068.

Luebke, J. I., and K. Dunlap. 1994. Sensory neuron N-type calcium currents are inhibited by both voltage-dependent and -independent mechanisms. *Pflügers Arch. Eur. J. Physiol.* 428:499–507.

Magnelli, V., A. Avaltroni, and E. Carbone. 1996. A single non-L-, non-N-type Ca^{2+} channel in rat insulin secreting RINm5F cells. *Pflügers Arch. Eur. J. Physiol.* 431:341–352.

Marchetti, C., E. Carbone, and H. D. Lux. 1986. Effects of dopamine and noradrenaline on Ca channels of cultured sensory and sympathetic neurons of chick. *Pflügers Arch. Eur. J. Physiol.* 406:104–111.

Meriney, S. D., D. B. Gray, and G. R. Pilar. 1994. Somatostatin-induced inhibition of neuronal Ca^{2+} current modulated by cGMP-dependent protein kinase. *Nature.* 369:336–339.

Plummer, M. R., D. E. Logothetis, and P. Hess. 1989. Elementary properties and pharmacological sensitivities of calcium channels in mammalian peripheral neurons. *Neuron.* 2:1453–1463.

Pollo, A., M. Lovallo, E. Sher, and E. Carbone. 1992. Voltage-dependent noradrenergic modulation of ω-conotoxin-sensitive Ca^{2+} channels in human neuroblastoma IMR32 cells. *Pflügers Arch. Eur. J. Physiol.* 422:75–83.

Rubinstein, R. Y. 1981. Simulation and the Monte Carlo Method. John Wiley and Sons, New York.

Shen, K. Z., and A. Surprenant. 1991. Noradrenaline, somatostatin and opioids inhibit activity of single HVA/N-type calcium channels in excised neuronal membranes. *Pflügers Arch. Eur. J. Physiol.* 418:614–616.

Swandulla, D., E. Carbone, and H. D. Lux. 1991. Do calcium channel classifications account for neuronal calcium channel diversity? *Trends Neurosci.* 14:46–51.

Toselli, M., and V. Taglietti. 1994. Muscarinic inhibition of high-voltage-activated calcium channels in excised membranes of rat hippocampal neurons. *Eur. Biophys. J.* 22:391–398.

Tsien, R. W., P. T. Ellinor, and W. A. Horne. 1991. Molecular diversity of voltage-dependent Ca^{2+} channels. *Trends Pharmacol. Sci.* 12:349–354.